# Measurement of Temperature and Velocity Vectors in a Combusting Environment Using Low-Cost Probes

**M. B. Khalil**[1]
Assoc. Mem. ASME

**E. G. Plett**
Professor.

Department of Mechanical and Aeronautical Engineering,
Carleton University,
Ottawa, Ontario, Canada K1S 5B6

*Radial traverses were made to measure temperature distributions and velocity vectors in an atmospheric pressure test combustor burning gaseous fuels with heating values in the low–medium range. Temperature was measured using an aspirated pyrometer probe. Velocity vectors were determined from measurements of a five-hole probe (a two-hole probe was used prior to the five-hole probe to determine whether the flow was directed upstream or downstream). The measuring traverse was carried out across the entire diameter at ten sections along the combustor (which was specially designed to allow in insertion of probes at the ten axial sections, through three holes at 120 deg from each other around the circumference). These measurements were repeated for ten runs that incorporated a variety of operating conditions of the combustor. Temperature measurements were validated by application of the first law of thermodynamics. Velocities were validated using the principles of conservation of mass and angular momentum. The analysis showed that temperatures can be measured to within 10°C in a combusting environment of gaseous fuels for which the temperature is in the vicinity of 1500 K, by an aspirated pyrometer. The axial velocity component can be measured to an average accuracy of 7.6 percent using five-hole probes. The radial component of velocity can be obtained within ±5 percent in most of the combustion space. The accuracy of measuring the circumferential velocity component could not be validated, partly because it was extremely small. Also, in order to validate it, some independent means of establishing its origin is needed. In this case, due to the lack of precision in fabricating the combustor and the holes for air admission, as well as due to the extremely small value of this component in the present study, it was not possible to establish the reliability of the measured values. The study recommends the use of aspirated pyrometers and five-hole probes in a combusting environment, provided that the yaw angle does not exceed 60 deg and the three components of velocity have comparable magnitudes. The probes should be made as small as possible and frequent purging should be practiced in their operation to avoid errors due to blockage of probes' passages by water or dust particles. These probes were chosen for this application because of the ease with which they can be used, as well as for cost considerations.*

## Introduction

Evaluation of the performance of combustors and combustion equipment requires the determination of the values of some thermodynamic and flow properties, such as temperature and velocity. The accuracy of measuring these quantities determines the level of accuracy of evaluating the performance of the combustor under consideration.

Probes inserted into the flow to measure temperature and velocity have been used longer than any other means for determining such quantities. Such probes, however, by their very nature, produce errors in the flow properties due to the disturbances resulting from their insertion. The area through which the flow passes changes due to the presence of probes resulting in errors in measuring static pressure. Also, in recirculating flows, the disturbance resulting from probes' insertion may travel upstream and change the entire flow behavior from that of the undisturbed flow. In some combusting flows, probe materials might act as a catalyst (or as a chemical sink for some species) for the chemical reaction and thereby change the reaction kinetics of the flow. These disadvantages, however, do not outweigh the usefulness of appropriate probes as a

[1]Present address: Asecor Ltd., Manotick, Ontario, Canada.

Contributed by the Gas Turbine Division of the The American Society of Mechanical Engineers and presented at the 32nd International Gas Turbine Conference and Exhibit, Anaheim, California, May 31–June 4, 1987. Manuscript received at ASME Headquarters February 6, 1987. Paper No. 87-GT-91.

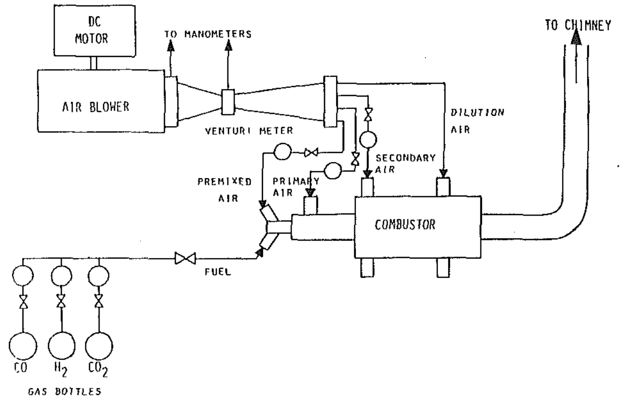


Fig. 1 Test rig layout

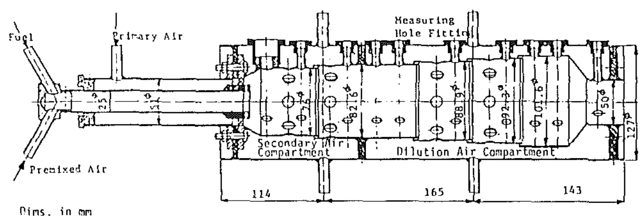


Fig. 2 Cross section of combustor assembly

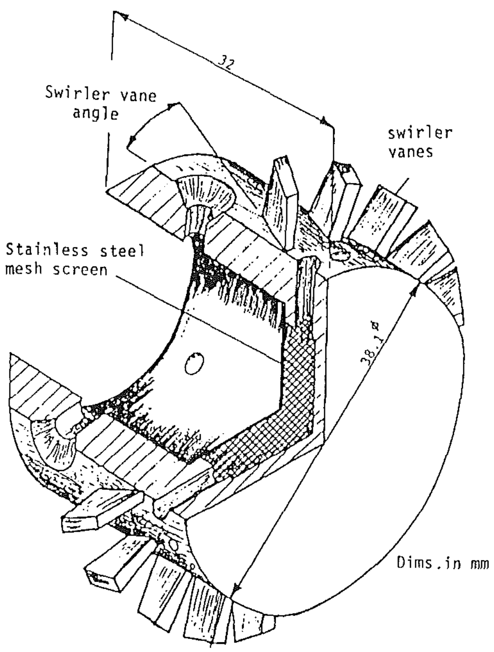


Fig. 3 Swirler-injector piece

reasonably accurate means of experimental measurements, since they are easy to use and of low cost compared to other more sophisticated means of measurements.

Experience in applying probes for flow measurements has resulted in improved probe designs, and therefore increased accuracy of their measurements. It is generally recommended that the smallest possible probe be used and the materials that might react with the flow be avoided [1].

The design and pertinent features of the probes used to measure temperatures and velocity vectors are described with sample results of the measurements given. The validity and accuracy of these measurements are evaluated in terms of their conformity to the conservation laws. The approach used in applying the conservation laws is outlined in the paper.

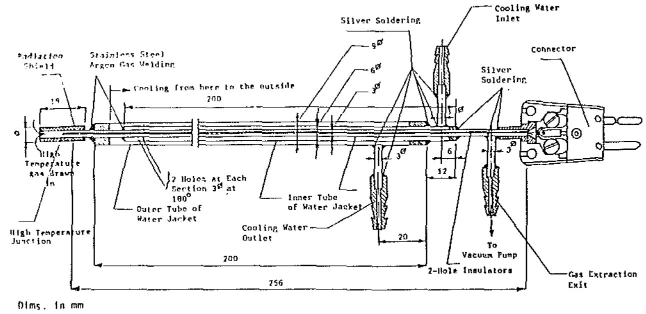


Fig. 4 Details of suction pyrometer

## Experimental Setup and Instrumentation

**Test Rig.** The experimental setup consisted primarily of a test combustor, fuel supply, and air supply (Fig. 1). The combustor was designed to allow insertion of probes into the combustion space through three holes spaced 120 deg apart, located at ten axial sections along the combustor. Air was admitted separately at the four zones of the combustor (premixed, primary, secondary, and dilution), with a typical distribution of air among the zones of 10 percent premixed, 10 percent primary, 40 percent secondary, and 40 percent dilution. Several other features in the design of the combustor can be found in [2]. The exit section of the combustor was connected to the laboratory's exhaust system.

Figure 2 shows a cross-sectional drawing of the combustor assembly and Fig. 3 shows a schematic view of the swirler-injector piece mounted in the combustor. The fuel used for this investigation was supplied by blending its constituents (to resemble low-medium heating value gas) from commercial gas bottles. The three components of the fuel, CO, $CO_2$, and $H_2$, were metered separately before being mixed and admitted to the combustor. The air needed for combustion was supplied by a centrifugal blower of capacity of up to 1857 $m^3/h$ at 3100 rpm. The blower was driven by a variable speed d-c motor, which provided a means of controlling the air flow rate. The total air flow rate was measured by a venturi meter mounted on the exit flange of the blower.

The air leaving the venturi was divided into two parts. The first part was directed to flow through six flowmeters en route to being admitted to provide the premixed, primary, and normally the secondary air. The second part was normally directed to provide the dilution air. The design of the combustor allowed for changing the proportion of air admitted at the various zones. The air flow rate to the dilution zone was determined by subtracting the summation of the flow through the six flow meters from the total air flow rate through the venturi meter.

**Aspirated Pyrometer Probe.** A radially traversing aspirated pyrometer probe was used to measure the temperature at the ten axial measurement sections. The probe was made of stainless steel with all welds in the flame region performed in argon (inert gas) atmosphere. The probe was water cooled to withstand the high temperature of the combustion gases. The probe surface temperature was maintained below 400°C (the safe operating temperature of stainless steel for this application). Figure 4 shows a cross-sectional drawing of the details of the probe. The thermocouple was made of platinum–platinum 13 percent rhodium (type R) wires, with a diameter of 0.2 mm. A suction pump was used to draw the high-temperature gases over the hot junction of the probe, through the ceramic shield. The thermocouple wires, insulators, and ceramic shield were supplied by Omega Engineering Inc.

It should be noted that the cooling of the suction pyrometer

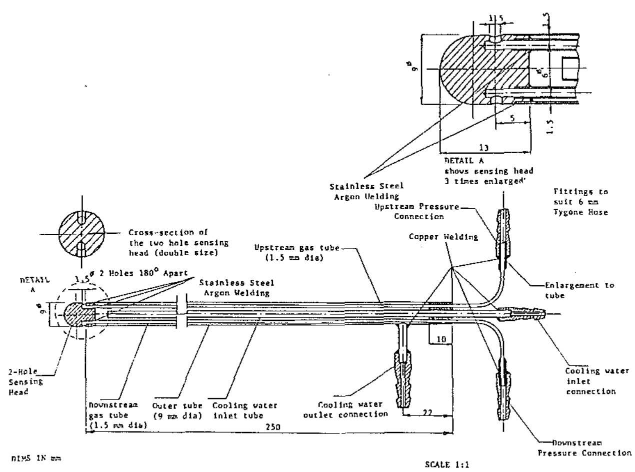


Fig. 5 Two-hole probe

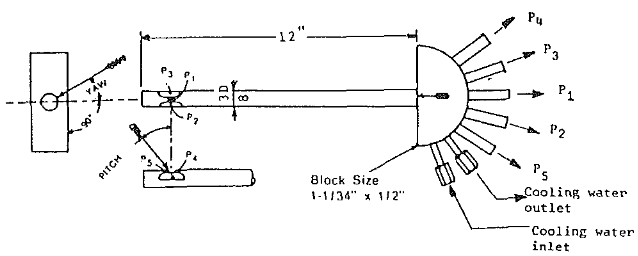


Fig. 6 Layout of the five-hole probe: main dimensions, pressures, and angles

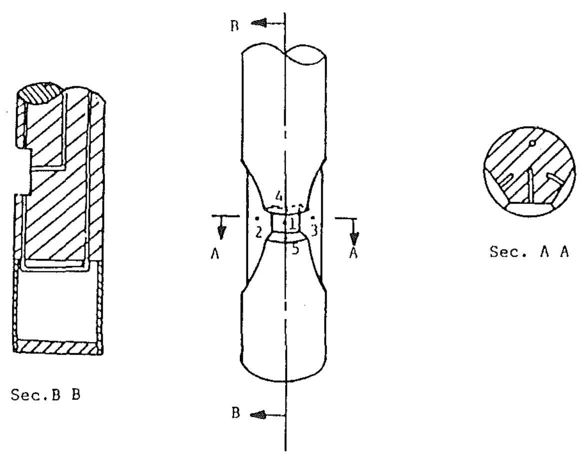


Fig. 7 Detail of five-hole probe tip

occurred in the portion of the probe that had the stainless steel jacket, and that the hot junction was in a region that was not cooled, but was surrounded by a ceramic radiation shield. Therefore, the probe should give the true reading of the local gas temperature without being affected by cooling of the probe surface or radiation to the cold liner walls. Appendix A contains a brief description of how the aspirated pyrometer probe was used to measure the gas temperature in the combustion region during this study.

It should also be mentioned here that the ceramic shield mounted on the aspirated pyrometer probe did not experience any noticeable deterioration in its mechanical properties over the period of this study (which extended over a period of two years, corresponding to service of about 500 h). This may be attributed to the precaution taken of allowing the cooling fluid to flow through the probe before it was inserted into the combustion space, which helped to reduce the thermal stresses resulting from rapid expansion of the metal parts near the joint where the ceramic shield is attached. It is advisable, in this context, to apply the "ceramic cement," to hold the ceramic shield attached to the metal portion of the probe, as close as possible to the end of the cooling jacket of the probe to avoid excessive thermal stresses that could cause crumbling of the ceramic radiation shield. Another factor that may have contributed to the life of the aspirated pyrometer probe was the clean gas combustion of this study. Purging with compressed air or nitrogen might be required in a slagging environment such as encountered with burning of liquid or solid fuels. Using steam as a coolant medium can also help in this case to prevent solidification of the fuel droplets or particles in the probe passages, because of the higher temperature allowed.

**Two-Hole Probe.** The two-hole probe was needed to determine the flow direction (i.e., up- or downstream) and to identify the recirculation zone in the combustion space. This is necessary because the five-hole probe cannot distinguish whether the flow is traveling upstream or downstream. Figure 5 shows a cross-sectional drawing of the two-hole probe that was designed and fabricated for this work. The probe simply has two holes located 180 deg apart around its circumference, with which it identifies the flow direction by allowing the pressure differential across the two holes to be measured, while the two holes are aligned parallel to the combustor axis. This probe was also made of stainless steel and was water cooled to withstand the high temperature inside the combustor.

**Five-Hole Probe.** A stainless steel, water-cooled, five-hole probe manufactured by United Sensors and Control Corporation (type DA-375) was used to obtain the velocity vector at the designated measurement sections along the combustor. Figure 6 shows a schematic drawing of the layout and dimensions of the probe, and Fig. 7 shows the details at the measuring tip of the probe. The five holes were located on a prism-shaped section in such a manner as to allow for measuring of the yaw angle, pitch angle, static pressure, and total pressure. The probe had its measuring tip along its stem, which simplified its insertion into the combustion space. The probe was rotated about its axis until the pressure difference ($P_2 - P_3$) was zero to allow measurement of the yaw angle by a protractor whose center was at the probe axis attached to the manual traverse unit. The location of the measuring tip along the probe stem allowed for a nulling operation of the probe without introducing error with respect to the top location, relative to the position where the measurement was required.

The procedure followed in measuring the velocity vector in the combustor region with the two-hole and five-hole probes is summarized in Appendix A. It should be mentioned that the five-hole probe was calibrated by the manufacturer and the calibration was checked before using it in this work. The check of the calibration was carried out using a setup consisting of an air supply, a plenum chamber with a nozzle attached, and the five-hole probe mounted on a device that allowed three degrees of freedom to the probe axis. Further detail can be found in [2], relating both to the calibration of the five-hole probe and to its use in conjunction with the two-hole probe.

## Evaluation of Measurements

**Temperature.** Experiments were carried out on the test combustor with a range of operating conditions while making radial traverses of measurements of temperature and velocity vector, at each of the ten measuring sections located along the combustor [3]. A gas sample was taken from the gases flowing through the aspirated pyrometer for gas analysis. However, due to the limited sensitivity of our gas partitioner (Fisher 1200), the analysis was limited to $CO_2$, $N_2$, $H_2$, $O_2$, and CO.

**Table 1 Summary of parameters considered for the various runs of the study**

| Run # | Swirler vane angle | $\dot{m}_f$ | HV | HV | Fuel Composition | | | $\dot{m}_{air}$ | Air Percentage at Various Zones %• | | | | A/F |
|---|---|---|---|---|---|---|---|---|---|---|---|---|---|
| | ° | kg/h | MJ/m$^3$ | MJ/kg | CO% | $CO_2$% | $H_2$% | kg/h | Pmd | Pri | Sec | Dil | kg/kg |
| 1 | 60 | 1.995 | 10.89 | 15.13 | 45.6 | 9.2 | 45.2 | 76.08 | 10 | 10 | 40 | 40 | 38.14 |
| 2 | 60 | 1.995 | 10.89 | 15.13 | 45.6 | 9.2 | 45.2 | 76.08 | 10 | 10 | 26.7 | 53.3 | 38.14 |
| 3 | 60 | 1.995 | 10.89 | 15.13 | 45.6 | 9.2 | 45.2 | 76.08 | 10 | 10 | 53.3 | 26.7 | 38.14 |
| 4 | 60 | 2.394 | 10.89 | 15.13 | 45.6 | 9.2 | 45.2 | 76.08 | 10 | 10 | 40 | 40 | 31.78 |
| 5 | 60 | 1.336 | 10.89 | 15.13 | 45.6 | 9.2 | 45.2 | 50.72 | 10 | 10 | 40 | 40 | 38.14 |
| 6 | 60 | 3.73 | 7.68 | 7.43 | 32.2 | 36.2 | 31.6 | 76.08 | 10 | 10 | 40 | 40 | 20.4 |
| 7 | 60 | 4.079 | 6.14 | 5.16 | 25.7 | 49.0 | 25.3 | 76.08 | 4 | 10 | 43 | 43* | 18.6 |
| | | | 6.62 | 5.61 | 27.7 | 44.9 | 27.4 | | | | | | |
| 8 | 0 | 1.995 | 10.89 | 15.13 | 45.6 | 9.2 | 45.2 | 76.08 | 4 | 10 | 43 | 43 | 38.14 |
| | | 1.336 | | | | | | | | | | | 56.95 |
| 9 | 30 | 1.336 | 10.89 | 15.13 | 45.6 | 9.2 | 45.2 | 76.08 | 4 | 10 | 43 | 43 | 56.95 |
| 10 | 45 | 1.336 | 10.89 | 15.13 | 45.6 | 9.2 | 45.2 | 76.08 | 4 | 10 | 43 | 43 | 56.95 |

* *This is the final air distribution(2).*
• Pmd = Premixed, Pri = Primary, Sec = Secondary, Dil = Dilution

**Table 2 Results of average temperature at first section of the combustor as calculated from energy balance and measurements of aspirated pyrometer**

| Method of obtaining av. temp. | Run # 1 | 2 | 3 | 4 | 5 | 6 | 7 | 8 | 9 | 10 |
|---|---|---|---|---|---|---|---|---|---|---|
| Energy balance | 1210 | 1210 | 1210 | 1206 | 1200 | 755 | 851 | 1117 | 1117 | 1076 |
| Measurements of aspirated pyro. | 1219 | 1218 | 1200 | 1198 | 1190 | 747 | 841 | 1107 | 1110 | 1170 |

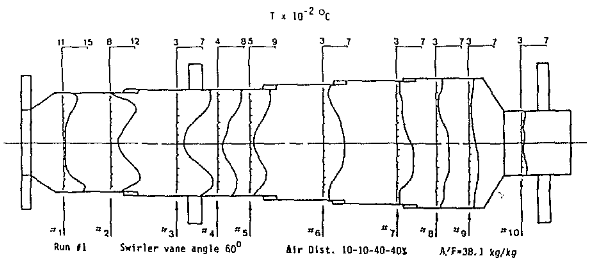


**Fig. 8 Radial profiles of temperature along the combustor for run No. 1**

The minimum concentration that could be measured with this gas chromatograph was 0.01 percent for CO and 0.05 percent for $H_2$ (by volume). Therefore, detailed gas analysis was not included as a part of this study.

Table 1 gives a summary of the operating conditions for the ten runs used in this investigation. Due to space limitations and for the sake of brevity, only samples of the results are given in this paper. Further details of the results may be found elsewhere [2, 3].

The temperature indicated by a thermocouple placed in a gas stream is its own temperature, which is the resultant of the various heat transfer modes bearing on the thermocouple junction [4, 5]. Errors in the measured temperature arise due to radiation and conduction heat exchange between the hot junction, the thermocouple wires, and the surroundings [4]. The aspirated pyrometer probe compensates for conductive heating by the gas as it passes over the hot junction, and also by shielding the hot junction to reduce the temperature difference between the junction and the surroundings, thereby reducing radiative losses. Conductive heat losses are minimized if fine wires are used for the thermocouple.

Chedaille and Braud [6] showed that the error due to the suction velocity in measuring the static temperature (rather than the total temperature) is less than 7°C at a suction velocity of 250 m/s. Since the suction velocity during this work was maintained at less than 50 m/s, it is implied that the error due to suction velocity was less than 7°C. It was found by Khalil et al. [4] that the effect of suction at the probe tip is limited to a sphere of 3 mm diameter at a suction velocity of 250 m/s. Therefore, the temperature measured by the suction pyrometer is considered to be representative of the value at the junction position. Aspirated thermocouples have a reasonably fast response (0.5 min), provided that a fine wire is used for the thermocouple. Some advantages of using aspirated pyrometer probes for measuring temperature in a combusting environment are enumerated elsewhere [2–6].

Figure 8 shows a sample of temperatures measured at the various sections along the combustor during run 1. The shape of the temperature profiles along the combustor agrees with previously obtained profiles from experimental and theoretical studies. The temperature profiles illustrate the effect of the boundaries and are representative of the expected temperatures at the location of the measurements in the combustor [7].

Errors in measuring the temperature of a combusting flow are expected to be higher near a flame zone (or at regions of very high temperature) due to the increase of heat loss. Therefore, it was decided to perform a check on the validity of the temperature measurements at the first section of the combustor. The procedure followed to compute the average temperature at the first section from flow rates, radiative heat losses, and the energy content of the fuel, using an energy balance, is given in Appendix B.

Following the procedure of Appendix B, for the ten runs of this investigation (Table 1 gives the operating conditions during the runs), the computed average temperatures from energy balances and from temperature measurements are given in Table 2. The table shows that the maximum difference between the measured and computed temperature was 10°C, with the temperature in the range of 1500 K in the first section. This is considered as excellent accuracy in measuring the temperature by an aspirated pyrometer probe.

**Velocity.** Due to the lack of sensitivity of the conventional Pitot tube to flow direction in measuring the velocity vector, attention has switched to the use of multihole probes. The first detailed description of the application of the five-hole probe was given by Lee and Ash [8]. Multihole probes have since then been used in a wide variety of investigations (see [2] for a complete bibliography).

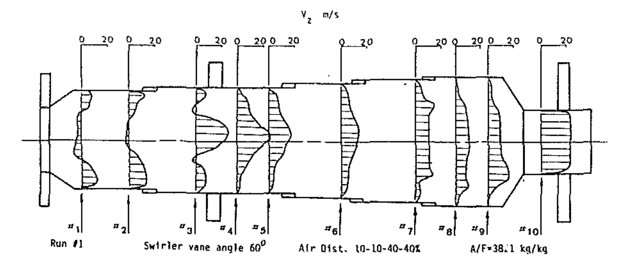


**Fig. 9 Radial profiles of axial velocity along the combustor for run No. 1**

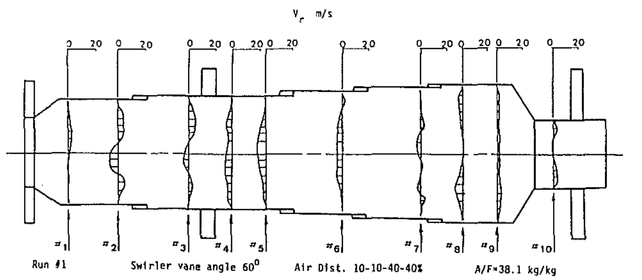


**Fig. 10 Radial profiles of radial velocity along the combustor for run No. 1**

**Table 3 Percentage difference in mass flow rate between values obtained from integration over section area and values obtained from inlet flow rates and open hole area, with the second value as the base value**

$\Delta\dot{m}\% = \{(\dot{m}_{\int} - \dot{m}_h)/\dot{m}_h\} \times 100$

| Run # \ Sec. # | 1 | 2 | 3 | 4 | 5 | 6 | 7 | 8 | 9 | 10 | Abs. av. |
|---|---|---|---|---|---|---|---|---|---|---|---|
| 1 | -10.3 | 4.0 | -4.6 | 18.2 | -1.2 | 1.7 | 16.8 | -0.5 | 8.1 | 2.5 | 6.8 |
| 2 | -2.9 | -8.9 | -11.4 | 8.4 | 20.2 | 0.8 | -5.5 | -6.0 | 10.3 | 2.2 | 7.7 |
| 3 | 4.6 | -12.9 | -0.4 | 21.8 | 17.9 | 2.1 | 11.0 | 4.8 | -2.5 | -0.2 | 7.8 |
| 4 | -8.6 | -13.1 | 1.0 | 8.0 | 2.0 | 3.0 | 3.6 | 4.2 | 15.0 | -2.5 | 6.1 |
| 5 | -2.7 | -5.2 | -15.6 | 43.5 | 10.0 | 13.5 | 0.2 | 0.0 | 14.8 | -2.0 | 10.8 |
| 6 | 2.9 | -2.9 | -6.1 | 1.3 | 2.0 | 1.4 | 4.6 | -0.9 | 1.5 | -0.7 | 2.4 |
| 7 | 3.7 | -14.9 | 7.6 | -7.1 | 3.1 | 8.4 | 3.7 | 3.0 | -0.3 | -1.5 | 5.3 |
| 8 | 24.5 | -14.6 | -15.9 | 4.8 | 2.0 | 6.3 | 3.9 | 18.7 | 16.8 | -1.8 | 10.9 |
| 9 | 7.7 | -13.7 | -12.1 | 10.1 | -8.1 | 4.8 | 4.5 | 14.4 | 10.8 | -2.0 | 8.8 |
| 10 | -4.1 | -23.1 | -6.7 | 1.2 | 7.4 | 4.5 | 10.2 | 19.5 | 11.8 | 0.8 | 8.9 |
| Abs. av. | 7.2 | 11.3 | 8.1 | 12.4 | 7.4 | 4.7 | 6.4 | 7.2 | 9.2 | 1.6 | 7.6 |

The accuracy of determining the velocity vector depends on the accuracy of measuring the required pressure differences by the five-hole probe, namely $(P_1 - P_{atm})$, $(P_2 - P_3)$, $(P_1 - P_2)$, and $(P_4 - P_5)$. The use of the five-hole probe in the nulling mode requires rotating the probe (about its axis) until $(P_2 - P_3)$ is zero, and the yaw angle is determined from the protractor reading in the manual traverse unit. The pressure differences were measured by a group of inclined manometers and a Hook gage manometer, which was equipped with a micrometer for more accurate reading of small pressure differences. The accuracy of reading the inclined manometers ranged from ±1.5 to ±4 percent. The Hook gage manometer is accurate to within 0.025 mm of water, hence its accuracy depends upon the value to be measured.

Operating the five-hole probe in the nulling mode improves the accuracy that can be achieved with the probe [9]. This is due to the simple manner of obtaining the yaw angle without the need for calibration. Frequent purging of the probe with compressed air or nitrogen [10] during measurements helps to remove any blockage in the passages leading to the manometers and thereby avoids a possible serious source of error.

An error analysis of measurements made with a five-hole probe by Gouldin [1] predicted errors to be less than 2 deg in yaw angle, 0.2 deg in pitch angle, and 3.5 percent in total pressure. Chue [11] and Dau et al. [12] found the accuracy in measuring static and dynamic pressure coefficients to be within 2–5 percent, and about 2 deg for pitch angle and 3–10 deg for yaw angle. Rhode et al. [13] estimated an accuracy of 5 percent for most measurements of five-hole probes, but it could reach 10 percent in regions of low velocity. The circumferential velocity component is expected to suffer the most in terms of accuracy due to its small value. Vu and Gouldin [14] found that five-hole probe measurements agree to within 2 percent with hot-wire anemometer results in regions of low turbulence levels and low velocity gradients. The difference, however, increased to 10 percent where turbulence and velocity gradients were higher.

The approach followed in this investigation to assess the accuracy of the velocity measurements by the five-hole probe was to apply the conservation principle pertinent to each component and to determine to what degree the measurements conform to the principle. The following sections describe the evaluation procedure for the three velocity components.

*Axial Component of Velocity.* Figure 9 shows a sample of the results of the axial velocity component plotted at the ten measuring sections along the combustor for run No. 1. In order to evaluate the accuracy of these results, the axial mass flow rate was computed, based on measured velocities, at all the measuring sections for the ten runs of this investigation. Appendix C gives a brief description of the procedure that was followed to interpret the results of this exercise in terms of the level of discrepancy in the axial velocity values at the various sections, upon application of the law of conservation of mass at these sections.

The results obtained upon application of the procedure of Appendix C for all sections for all runs given in Table 1 are summarized in Table 3. The last column and row of Table 3 contain the absolute mean value of the percentage difference in one run through all sections and in any section from all runs, respectively. The results in the table show a close agreement between the two approaches of calculating the mass flow rate at the combustor sections, especially near the exit section, where the difference was ±2.5 percent. It should be noted that while the difference seems to be higher at some sections, the absolute average for the ten runs is less than 7.6 percent. The maximum absolute average percentage difference for any run is about 10.9 percent. The maximum absolute average percentage difference at any section from all the runs is about 12.4 percent (at section 4). What might have contributed to the magnitude of error at this section is the fact that it is located between the secondary and dilution zones and if air leaked from one of these compartments into the other (Fig. 2), it would have produced an immediate error in the method of evaluating the accuracy of the measurements. The variation of these differences from one section to the other reveals that generally, for sections upstream of and including section 3, the mass flow rate calculated from velocity measurements is less than what is expected from the input air admitted up to that section. The opposite trend is found for sections 4–9. On the average, the mass flow, computed based on the axial velocity component obtained from measurements with the five-hole probe, agrees very well with the value deduced based on input mass flow rate.

*Radial Component of Velocity.* Figure 10 shows the radial profiles of the radial velocity component at the ten sections for run No. 1 as a sample of results. Examination of this figure and similar figures for other runs showed that there is a value for the radial velocity component that exists along the entire section even at the axis, with no change of sense for some profiles. At first glance, this could imply a discrepancy in the results due to the fact that such profiles require a source or sink flow at the combustor axis. However, the discrepancy might be alleviated if the gradients of the velocity vector com-

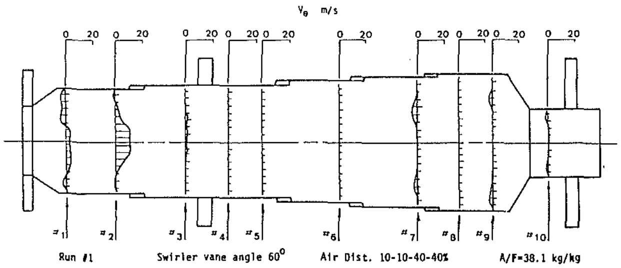


**Fig. 11 Radial profiles for circumferential velocity along the combustor for run No. 1**

ponents in the other two directions are large enough to compensate for the radial velocity component near the axis.

In order to assess the validity of the distributions obtained, the profiles that seemed suspect were examined in light of the continuity principle applied to a control volume in the vicinity of the combustor axis. This also indirectly checked the axial and circumferential velocity components. A semicylindrical control volume was adopted, for this purpose, at the combustor axis between adjacent measuring sections. The diameter of the control volume was taken to be equal to its axial length. This shape of the control volume allowed for consideration of the effect of the three velocity components as well as the effect of the lack of symmetry about the combustor axis. Appendix D outlines the procedure followed to do this.

Application of the procedure outlined in Appendix D to the radial velocity profiles at sections where they seemed unrealistic resulted in an average value of 3.5 percent discrepancy in the conformity of the results to the continuity equation. This means that the results of the radial velocity component are physically acceptable since, when used in mass flow computations, they provide close agreement with the other independently measured mass flows, for which the accuracy has been established as acceptable.

It should be pointed out that the accuracy of the calculations of the radial component of velocity is dependent on the accuracy of obtaining the pitch angle, which depends on the pressure difference $(P_4 - P_5)$ as obtained from the five-hole probe. At very low velocities (less than 1 m/s) the accuracy in measuring $(P_4 - P_5)$ is reduced due to the limitations of the manometer reading accuracy.

*Circumferential Component of Velocity.* The presence of a swirler in the flow passage of the primary combustion air produces a circumferential component for the velocity vector, for flow near the primary zone, in the same direction as that of the swirler vanes. This component should decay to zero near the combustor axis and more generally as the flow proceeds downstream toward the combustor exit. It should be near zero over the entire exit section.

Figure 11 shows, as an example, the radial profiles of the circumferential velocity component plotted at the various sections along the combustor for run 1. The circumferential velocity profiles presented in the figures, as well as those obtained for other runs, do not conform to the above-mentioned behavior and even, at most of the sections, show a negative value (opposite to the twist of the swirler vanes).

In order to check the validity of the circumferential velocity profiles, the axial flux of angular momentum was calculated at all sections for all runs, similar to calculating the mass flow rate, by integrating the required quantity over the section area. The effects of shear stresses and pressure differences on the axial flux of angular momentum were not taken into consideration, however. The axial flux of angular momentum supplied at the combustor head via the swirler was compared with the value obtained from integration over each section of the combustor. The procedure for doing this is summarized in Appendix E.

**Table 4 Difference in axial flux of angular momentum from calculations at the various sections and the inlet value to the combustor**

$(G_{\phi s} - G_{\phi i}) \times 10^4$ Nm

| Run # \ Sec. # | 1 | 2 | 3 | 4 | 5 | 6 | 7 | 8 | 9 | 10 |
|---|---|---|---|---|---|---|---|---|---|---|
| 1 | -1.65 | 1.07 | 1.84 | -0.06 | -1.82 | 0.078 | 5.58 | -2.86 | -2.12 | 1.49 |
| 2 | -1.25 | -1.74 | -1.85 | -0.52 | -1.19 | -0.26 | 0.94 | 2.11 | 3.21 | 0.19 |
| 3 | -1.06 | -0.97 | -0.50 | -1.58 | -1.81 | 3.12 | -0.64 | 4.95 | 2.36 | 1.88 |
| 4 | -6.08 | -0.76 | -7.10 | 0.43 | 1.03 | 0.11 | 2.97 | 2.51 | 1.75 | 6.12 |
| 5 | -0.38 | 0.63 | 0.08 | -1.00 | -0.60 | -0.32 | 0.68 | 0.12 | -0.05 | -0.58 |
| 6 | 0.64 | 0.47 | 0.53 | -0.31 | -0.99 | -0.49 | -0.87 | -1.83 | 3.15 | 1.33 |
| 7 | -0.91 | -0.36 | -0.58 | -1.36 | -1.07 | -0.97 | 0.11 | 0.66 | 1.56 | 1.11 |
| 8 | 0.19 | 1.31 | 0.90 | -0.82 | -1.20 | 0.43 | 0.27 | 1.74 | 1.92 | 2.23 |
| 9 | 0.02 | -0.04 | -0.22 | -3.73 | -0.69 | 0.87 | 1.79 | 0.64 | 1.38 | 2.38 |
| 10 | 0.17 | 0.18 | 0.15 | -0.44 | -0.39 | -0.11 | 3.76 | 3.30 | 0.80 | 1.91 |

Table 4 presents the resulting difference in axial flux of angular momentum $(G_{\phi,s} - G_{\phi,i})$ in Nm, where $G_{\phi,s}$ = axial flux of angular momentum calculated by integration of experimental results at the sections; $G_{\phi,i}$ = inlet axial flux of angular momentum generated by the swirler. The results in Table 4 are given for all sections and all runs after following the procedure described in Appendix E. These results show that the two computations do not agree with each other at most of the sections. The results even suggest that the direction for the circumferential velocity may have been measured opposite to the direction offered by the swirler.

It should be noted, however, that the values of the axial flux of angular momentum at the combustor inlet are generally less than $8 \times 10^{-5}$ Nm (compared to the value of $3.4 \times 10^{-2}$ Nm for the product of axial momentum and combustor radius). If, during fabrication of the combustor, the holes that admit the secondary and dilution air were 5 percent off the radial direction (due to misalignment of the drill for example), that would result in an axial flux of angular momentum of $1.2 \times 10^{-5}$ Nm at the third measuring section and higher values at downstream sections. The same can be said about the holes that admit the fuel-air mixture. If this misalignment was in the direction opposite to the twist of the swirler vanes, it would result in a negative circumferential component. Therefore, a 5 percent error in fabrication of the combustor could produce a value of the axial flux of angular momentum of the same order of magnitude as the value at the combustor inlet due to the swirler vanes. This can be one of the main reasons for the large discrepancy in the circumferential velocity measurements.

The fact that pressure difference and shear stress effects, particularly in the recirculation zone, were not accounted for in calculating the axial flux of angular momentum, could contribute to the difference obtained between the two values, especially with large temperature gradients in the combustion zone, which directly affect the density needed in the mass balance computation. Since the circumferential component was an order of magnitude (at least) less than the axial velocity component, when using the two values in a conservation equation to check the validity of the circumferential component, a small fractional uncertainty of the axial component could appear to produce a much larger fractional error in the circumferential component. Such small values of the circumferential velocity resulted in attempts to measure a pressure difference $(P_4 - P_5)$ of less than 0.025 mm water, where the manometer reading accuracy is very marginal.

Since no other approach was available to prove or justify the circumferential velocity profiles, they were shown [2] as dotted lines to convey this uncertainty.

## Summary and Conclusions

Temperature measurements using an aspirated pyrometer probe showed very good accuracy in the combustion environment, which included regions with temperatures of up to 1500 K . The maximum difference between the measured value and the value that was expected based on energy conservation considerations was less than 10°C.

After evaluating the performance of the five-hole probe in measurements of the velocity vector in highly turbulent combusting flows (that contain a recirculating region), it was concluded that the measurement accuracy was quite satisfactory for the axial velocity and reasonable for the radial component, as verified by application of the continuity principle. The circumferential component could not be proven satisfactory (or otherwise). The variation in the reliability by which the five-hole probe responds to the three components is mainly due to the variation in their magnitudes, since the uncertainty in reading a manometer is approximately the same whether the reading is 1 cm or 0.0025 cm of water.

In order for the overall reliability of measurement of three velocity components with a five-hole probe as used in this study to be uniform, the three components would, in general, have to be of comparable magnitude to each other and none should be less than 10 m/s. Lower velocities will require high-precision manometers which, if the pressure difference is below 0.0025 cm of water, becomes impractical, which means that these low values cannot be accurately measured even with inclined (or Hook's) manometers.

The accuracy of the five-hole probe for pitch or yaw angles beyond 40 deg is highly degraded and the probe should not be used beyond this angle. A five-hole probe requires calibration, which is normally done in flows that are uniform in velocity and homogeneous in temperature and composition. This raises the possibility of another source of error when a probe thus calibrated is used in the present study with its highly sheared flow. The five holes in the probe occupy a circle of about 5 mm diameter. Therefore, placing this probe in a flow that has large thermal, dynamic, and chemical composition gradients may lead to another source of error as each of these holes measures in fact a flow that is different from the others. This is in contradiction to the basic assumptions in the calibration of the probe, which assume a uniform homogeneous flow in order to facilitate the application of Bernoulli's equation to the flow between the mainstream and any of the holes. Variation of the gradient of density, for example, from one region to another, is not accounted for in a usual calibration of this type of probe.

The above statements imply that for this research, the measured values of the axial velocity could be taken as generally acceptable; the values of the radial velocity component are acceptable but with less certainty than the axial velocities. The circumferential velocity values, on the other hand, should be treated with caution. This, however, does not negate the usefulness of the low-cost five-hole probe as a tool that is easy to use for obtaining at least the most significant components of the velocity vector in a recirculating, combusting environment.

## Acknowledgments

This paper is based on the Ph.D. Thesis of M. B. Khalil. The research was supported in part by the Department of Energy, Mines, and Resources (EMR), Canada and by the Natural Sciences and Engineering Research Council of Canada (NSERC).

## References

1 Gouldin, F. C., "Probe Measurements in Multi-dimensional Reacting Flows," *Testing and Measurement Techniques in Heat Transfer and Combustion*, AGARD C. P. 281, 1980.

2 Khalil, M. B., "Investigation of Combustion Characteristics of Low-Medium Heating Value Gases in an Atmospheric Pressure Combustor," Ph.D. Thesis, Carleton University, Ottawa, Canada, Sept., 1984.

3 Khalil, M. B., and Plett, E. G., "Experimental Investigation of Parameters Affecting the Performance of an Atmospheric Pressure Test Combustor Burning Low-Medium Heating Value Gas," presented at the ASME Winter Annual Meeting, Anaheim, CA, Dec. 1986.

4 Khalil, M. B., El-Mahallawy, F. M., and Farag, S. A., "Accuracy of Temperature Measurements in Furnaces," *Letters in Heat and Mass Transfer*, Vol. 3, No. 5, 1976, p. 421.

5 Beer, J. M., and Chigier, N. A., *Combustion Aerodynamics*, Applied Science Publishers Ltd., London, 1972.

6 Chedaille, J., and Braud, Y., "Industrial Flames," in: *Measurements in Flames*, Vol. 1, IFRF, 1972.

7 Swithenbank, J., Poll, I., Vincent, M. W., and Wright, D. D., "Combustion Design Fundamentals," *14th Symposium (Int.) on Combustion*, 1973, p. 627.

8 Lee, J. C., and Ash, J. E., "A Three-Dimensional Spherical Pitot Probe," *Trans. of the ASME*, Vol. 78, Apr. 1956, p. 603.

9 Chigier, N. A., "Velocity Measurements in Vortex Flows," in: *Flow, Its Measurement and Control in Science and Industry*, Vol. 1, R. B. Dowdell, ed., Instrument Society of America, 1974.

10 Chigier, N. A., "Pressure, Velocity and Turbulence Measurement in Flames," in: *Flow, Its Measurement and Control in Science and Industry*, Vol. 1, R. B. Dowdell, ed., Instrument Society of America, 1974.

11 Chue, S. H., "Pressure Probes for Fluid Measurement," *J. of Progress in Aerospace Science*, Vol. 16, No. 2, 1975, p. 147.

12 Dau, K., McLeod, M., and Surry, D., "Two Probes for the Measurements of the Complete Velocity Vector in Subsonic Flow," *J. of the Roy. Aero. Society*, Vol. 72, No. 696, 1968, p. 1066.

13 Rhode, D. L., Lilley, D. G., and McLaughlin, D. K., "Mean Flow Fields in Axisymmetric Combustor Geometries With Swirl," *AIAA J.*, Vol. 21, No. 4, 1983.

14 Vu, B. T., and Gouldin, F. C., "Flow Measurements in a Model Swirl Combustor," *AIAA J.*, Vol. 29, No. 5, 1982, p. 642.

15 Reynolds, W. C., *Thermodynamics*, McGraw-Hill, New York, 1965.

# APPENDIX A

## Procedure for Measuring Temperature and Velocity Vector

### A 1 Temperature Measurement

1 The aspirated pyrometer (AP) was mounted into the manual traverse unit (obtained from United Sensor and Control Corp.).

2 The manual traverse unit (MTU) was fixed in place by a clamp at the section along the combustor, where the measurement was to be made, with the AP junction at the far end wall.

3 The suction pump was switched on and the temperature reading at steady state was recorded.

4 Using the linear vernier and the traverse scale, the AP was drawn radially out a distance of 5.0 mm and the new temperature reading was recorded.

5 The traverse was made across the diameter of the combustor for that measuring hole at that section; then the MTU (and AP) were moved to the second hole (at the same section) which is located 120 deg clockwise from the first hole, where the procedure was repeated.

6 The procedure was repeated again at the third hole of the section. The temperature at a given radial location was considered to be the average of the three readings on that side of the centerline, at that section.

7 The probe was then moved to another section, and the procedure repeated, until the entire combustor had been surveyed.

### A2 Velocity Vector Measurement

1 A complete traverse of the combustion space was carried out using the two-hole probe (mounted on the MTU) to identify the recirculation zone or the boundaries of the reversed flow.

2 The five-hole probe was mounted in the MTU, which in turn was fixed by a clamp at the combustion section where the

velocity vector determination was desired, with the tip of the probe at the far wall of the liner.

3 The five-hole probe was placed in accordance with the flow direction indicated by the two-hole probe, rotated about its axis until the pressure difference indicating the yaw angle became zero, which allowed the yaw angle to be obtained from the protractor reading of the MTU.

4 The three pressure differences (Fig. 6), which indicate the dynamic pressure difference, total pressure, and pitch angle, were recorded at this position.

5 The probe was then moved radially a distance of 5 mm, using the MTU, and directed in accordance with the reversed flow boundaries, where the above procedure was repeated.

6 When the probe readings were taken over the entire diameter of one section, the MTU (with the probe) was moved to the next hole 120 deg clockwise at the same section.

7 The procedure was repeated at this hole and the third hole at each section.

8 The procedure was followed at all sections along the combustor.

9 The velocity vectors were computed at each of the three holes at each section, from the pressure differences measured, on the basis of the probe calibration, after correcting for reduction of flow area due to probe insertion.

10 The velocity components were obtained from resolving the velocity vector in the three directions, namely axial, radial, and circumferential.

11 The average value of each of the components was obtained from the three readings at the three holes, for each radial position for each section along the combustor.

## APPENDIX B

### Calculation of the Average Temperature at the First Section of the Combustor

This appendix illustrates briefly the procedure of calculating the average temperature at the first section of the combustor for the various runs of this investigation. A more detailed description can be found in [2].

1 From fuel and air flow rates at the combustor first section, the average values (over the section) of the concentrations of the reactants and products are calculated with the help of gas analysis.

2 From the above calculated values for concentrations of reactants, the total enthalpy at combustor inlet is calculated as described in many texts dealing with thermodynamics of combustion (e.g., [15]).

3 Knowing the concentrations of various components at the first section, the relative amounts of chemical and sensible enthalpy are found.

4 The heat loss by radiation from the combustor surface up to the first section is estimated from knowledge of combustor design and the average surface temperature at the first section.

5 The net sensible enthalpy of the products of combustion at the first section is calculated knowing the total sensible enthalpy and subtracting the estimated radiative losses.

6 A temperature is found (usually by a trial and error procedure) that is consistent with the concentrations and net sensible enthalpy. This is the average temperature at the first section.

## APPENDIX C

### Procedure for Evaluation of the Accuracy of Results of the Axial Velocity Component

This appendix outlines a procedure for evaluating the accuracy of the results of axial velocity measurements as obtained from the five-hole probe. The details of the procedure can be found in [2]. The steps are as follows:

1 Compute the mass flow rate at each section of the combustor, for the run under consideration, as follows:

$$\dot{m}_s = \int_A \rho v_z dA$$

where

$\dot{m}_s$ = mass flow rate at the sections being examined
$\int_A$ = integration over the area of the section
$\rho$ = gas density
$v_z$ = axial velocity

The above integration was performed numerically using the method of trapezoids. The area increment was calculated from the mean radius between the relevant two measuring points and the increment of distance between these two measuring points. The density of the gas was calculated from the equation of state at the mean temperature after calculating the gas constant based on the gas composition.

2 The mass flow rate at each of the measuring sections ($\dot{m}_a$) was calculated from the mass flow rate of fuel and the amount of air admitted up to the section under consideration. The amount of air admitted through the holes for secondary or dilution air as well as through holes for film cooling can be estimated to be proportional to the open area up to the section under consideration as a fraction of the total area available for flow to pass through. This is assuming a constant discharge coefficient for all holes of a particular type at a particular zone or ring of the combustor.

3 The percentage difference in the mass flow rate as computed from steps 1 and 2 is calculated as follows:

$$\Delta\dot{m}(\text{percent}) = \frac{\dot{m}_s - \dot{m}_a}{m_a} \times 100$$

where

$\Delta\dot{m}$(percent) = percentage difference in mass flow rate
$\dot{m}_s$ = mass flow rate calculated from integration of axial velocity measurements × density along the section area
$\dot{m}_a$ = actual mass flow rate that is expected to occur at the section based on measured flow rates to the combustor and on the combustor design

## APPENDIX D

### Procedure for Evaluation of the Accuracy of Results of the Radial Velocity Component

Figure D1 shows a schematic drawing of the control volume at the combustor axis, which was used to apply the continuity equation to determine the accuracy of radial velocity measurements. Axial flow resulting from the axial component of velocity will take place only through the two semicircular ends of the control volume. Radial flow is possible only through the curved surface of the cylindrical control volume (ABFDCEA). Circumferential flow is possible only through the flat surface of the control volume (ABCD). The approach followed here was simply to determine the net mass flow rate to the control volume from the results of velocity measurements to determine how close to zero it is.

1 The axial mass flow rates at both ends are calculated over the area following the same procedure described in Appendix B, with the exception that the cross section is a semicircle and extends only to the diameter of the control volume.

2 The radial mass flow rate is calculated by averaging the values of the radial velocity components at the four corners A, B, C, and D, assuming linear variation and considering the

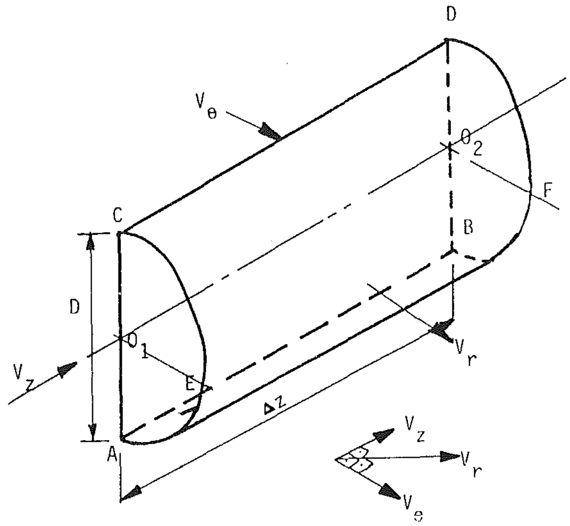


Fig. D1 Control volume at the combustor axis

resulting value to flow through the curved surface of the control volume.

3 The mass flow rate due to the circumferential component of velocity was estimated as follows: The circumferential velocity was averaged over AO1, O1C, BO2, and O2D. The average over CO1 and O2D was considered to flow through the area CDO2O1 and the average over AO1 and BO2 was considered to flow through the area ABO2O1.

## APPENDIX E

### Procedure for Evaluation of the Accuracy of Results of Circumferential Velocity Component Measurements

There are two bases for calculating the axial flux of angular momentum, which is conserved in swirling flows. Calculations are based on experimental measurements and on the swirler design and input flow rates. The procedure is carried out as follows:

1 The axial flux of angular momentum is calculated at any section of the combustor from the relationship

$$G_{\phi,s} = \int_A \rho v_z v_\theta r dA$$

where $v_\theta$ = circumferential velocity component. This step is to be carried out similarly to computing the mass flow rate at the combustor section, described in Appendix B.

2 The axial flux of angular momentum at the inlet to the combustor due the presence of a swirler is calculated from the following expression, given by Beer and Chigier [5]:

$$G_{\phi,s} = \int_{r_i}^{r_o} \rho v_z v_\theta 2\pi r^2 dr$$

where $r_i$ = inner radius of swirler: $r_o$ = outer radius of swirler.

If the axial velocity $v_z$ is assumed to be uniform over the range $r_i$-$r_o$, the circumferential velocity $v_\theta$ will be uniform because $v_\theta = v_z \tan\theta$ for straight vanes of angle $\theta$ to the combustor axis.

$$G_{\phi,i} = \int_{r_i}^{r_o} \rho v_z^2 2\pi r^2 dr \tan\theta$$

$$= 2\pi\rho v_z^2 \tan\theta \int_{r_i}^{r_o} r^2 dr$$

$$= 2/3\pi\rho v_z^2 \tan\theta (r_o^3 - r_i^3)$$

Substituting for $v_z$ from the mass flow rate through the swirler and the swirler open flow area (neglecting the thickness of the vanes),

$$G_{\theta,i} = \frac{1}{5\pi\rho}(\dot{m}_{pri})^2 \frac{r_o^3 - r_i^3}{(r_o^2 - r_i^2)^2} \tan\theta$$

where $\dot{m}_{pri}$ = mas flow rate through the swirler (primary air).

The values $G_{\phi,i}$ were calculated from the operating flow rate for the ten runs with the value of $\theta$ substituted corresponding to the swirler mounted during the run. The density was calculated assuming that the flow achieved a temperature of 300°C at the swirler exit section.

It should be mentioned here that $G_{\phi,i}$ can be computed from measurements of pressure drop and torque at the combustor inlet with fewer assumptions required. The operation of the combustor at atmospheric pressure and the separate admission of air to the combustor zones prevented us from following this route.